

Theory of high pressure hydrogen, made simple

Ioan B Magdău, Floris Balm and Graeme J Ackland

CSEC, SUPA, School of Physics and Astronomy, The University of Edinburgh, Edinburgh EH9 3JZ, United Kingdom

E-mail: i.b.magdau@sms.ed.ac.uk, gjackland@ed.ac.uk

Abstract. Phase I of hydrogen has several peculiarities. Despite having a close-packed crystal structure, it is less dense than either the low temperature Phase II or the liquid phase. At high pressure, it transforms into either phase III or IV, depending on the temperature. Moreover, spectroscopy suggests that the quantum rotor behaviour disappears with pressurisation, without any apparent phase transition [1]. Here we present a simple thermodynamic model for this behaviour based on packing atoms and molecules and discuss the thermodynamics of the phase boundaries. We also report first principles molecular dynamics calculations for a more detailed look at the same phase transitions.

1. Introduction

In 1935 Wigner and Huntington proposed a metallic modification of hydrogen as an atomic phase at high pressure. They calculated that metallisation would occur at about tenfold compression, which is remarkably close to modern estimates. They also quoted a transition pressure of 25GPa, which has proved over an order of magnitude too low, and has been widely ridiculed. This should stand as testament that calculated volumes are more reliable than pressures.

The experimental search for crystalline metallic hydrogen continues, and with numerous non-metallic phases reported, it has become clear that a different physical picture from Wigner and Huntington’s “atomisation begets metallisation” is required.

The structure of solid hydrogen up to 250GPa is now generally agreed upon. Phase I is a hexagonal close-packed molecular liquid. Here, the high-school picture of H₂ as a dumbbell molecule is misleading, because at low pressure H₂ behaves as a free molecular rotor, and the $J = 0$ quantum ground state is spherical. Hence, phase I can be thought of as simply close packing of spherical objects. As pressure is increased the molecules interact with each other and J ceases to be a good quantum number. At low temperature this leads to a “broken symmetry” Phase II, where the rotation has stopped. There have been numerous predictions for the crystal structure of this phase, which is normally regarded as a structure near to hcp in which molecular orientation is fixed. At high temperature, the melt line shows a maximum around 900K/70GPa[2, 3, 4]; if pressure is increased further the melting temperature drops, meaning the liquid is denser than the close-packed Phase I.

At high pressures, where the mechanical work of compression (PV) approaches the molecular binding energy, complex phases are observed. Theory predicts that these are based around a new motif - weakly bound molecules arranged into hexagonal trimers[5, 6, 7]. Distinct molecules are still observed, albeit with short-lived, weaker and longer bonds. In the low temperature “Phase III” all molecules are in such trimers, however, at high temperature

“Phase IV” appears to comprise alternating layers of trimers and relatively freely rotating molecules[6, 8]. If the proton motions are treated quantum mechanically, either by path integral sampling or through consideration of tunneling probabilities, the many-proton wavefunction attains $P6/mmm$ symmetry directly and the weak molecules manifest as a correlation in the proton wavefunction.

These phases can all be reproduced by considering classical protons interacting via forces calculated in the density functional theory. The calculated pressure and temperature phase boundaries depend on the details of the calculation which typically involve trade-offs between system size, exchange correlation treatment, pseudopotential fidelity, quantisation of nuclear motion and k-point sampling.

It is widely assumed that quantised proton motion and advanced treatment of exchange-correlation for van der Waals bonding are essential to describe the bonding[9]. So it is curious that the “quantum rotor” phase I is well explained by molecular dynamics using PBE and classical rotors[2]. Given that the melting point maximum was predicted by classical molecular dynamics simulation with remarkable accuracy, one has to believe that if those quantum effects are essential, they are exactly compensated by an incorrect piece of classical physics.

In this paper we examine what is the minimal physics required for an understanding of the hydrogen phase diagram. We do not aspire to obtain accurate pressures or temperatures, rather the questions to address are:

- (i) Is there a simple explanation for the mixed atomic-molecular phase IV?
- (ii) Does phase I comprise free rotors at all pressures?
- (iii) How does the melt become denser than the close-packed solid phase I?

2. A simple packing model

Despite the wide range of candidate structures reported from ab initio structure-search techniques[5, 10, 11], there are essentially three motifs that are sufficient to capture the physics of the phase diagram: rotating molecules, non-rotating molecules, and layers comprising short-lived molecules where the time-averaged, indistinguishable-atom positions form hexagonal layers. Structure search reveals numerous possible small distortions which molecular dynamics or path integral methods show are eliminated by elevated temperatures and/or quantum behaviour of the protons[7, 12, 13]. Our simple model for this considers three objects:

- S: Spherical molecules, which correspond to a $J = 0$ quantum rotor ground state, or a time-averaged classical free rotor. S objects have high volume and high internal entropy.
- R: Rod-like molecules, corresponding to the non-rotating type, with length similar to the diameter of S. R molecules have smaller volume than S, and zero internal entropy or energy.
- A: Spherical “atoms”, about half that of S. They have no internal entropy, and high internal energy due to the broken bond.

In our model, phase I comprises S-type objects, phase II R-type, phase III R-type (better packed, but elongated), phase IV is a binary mixture of A and S. The liquid contains S, R and A objects according to their Boltzmann weights. A packing fraction and an internal energy is assigned to each crystal structure. The total free energy of each phase is then the sum of the energies of the crystal and its component objects. We have considered other crystalline arrangements within the model, and the only competitive structure is close-packing involving a single H atom (labeled “Atomic” in figure 1).

We can model the hydrogen molecule as two spherical atoms with centers separated by about 0.74\AA . At atmospheric pressure, the density is $23\text{ cm}^3/\text{mol}$, (about 39 \AA^3 per molecule) indicating that the molecules are far apart compared to their bond length. At low pressure, hydrogen is extremely compressible, which implies that in this regime, close-packing of rigid spheres is not a

good approximation. The close-packed density for such S-objects, i.e. where the intermolecular distance becomes close to double the bohr radius, is reached at around 200GPa[8, 14, 15] which is where transitions to phase III and IV start to happen.

We have no explicit treatment of compressibility within a phase. This is because to calculate phase boundaries using the geometric model presented here requires only that the volume difference between competing phases is similar along the phase boundary (c/f figure 2). This breaks down for low pressures where an additional parameter is required (see supplemental).

The hcp structure has a packing fraction of 0.7405, which is maintained by an affine deformation to nonideal c/a by transforming spheres into oblate spheroids. Naively, one might expect a transformation directly from close-packed S to A, at a pressure which favours the smaller objects, however, a mixed S-A structure can have denser packing provides it adopts the, MgB_2 structure, $P6/mmm$, one of only two structures which has a lower free energy than hcp for binary hard spheres[16]. The time-averaged structure of SA_2 Phase IV is precisely this[6, 7].

Therefore the pressure stability of this apparently complex Phase IV can be attributed to efficient SA_2 packing. The temperature stabilisation of Phase IV vs III comes from the entropy of S objects. In molecular dynamics, it is observed that the atoms in phase IV form short-lived molecules, like our R-objects, so we assign a lower energy to IV the atomic close-packing phase objects.

The melting point maximum requires that the liquid has higher compressibility than the solid. In the model, liquid contains all three objects weighted by their free energy, so the increased population of smaller type R and A objects causes the liquid to become denser at high pressure.

The thermodynamic explanation for the phase transitions in this picture is:

- I \rightarrow II. Quadrupole-quadrupole interaction favours phase II. Pressure favours phase II due to R being smaller than S, despite inefficient packing of phase II to minimise EQQ. S-object entropy favours phase I.
- I \rightarrow IV. Pressure favours phase IV's denser AB_2 packing. S-object entropy favours phase I.
- I \rightarrow liquid. Entropy favours the liquid phase. Liquid has less efficient packing, but contains smaller objects, especially at high pressure. So pressure initially favours I, but subsequently favours the liquid.
- III \rightarrow IV. Entropy gain from S-objects and volume decrease due to efficient AB_2 packing.

PIMD calculations have shown that zero point motion reduces all transition temperatures, so nuclear quantum effects can be included as an offset of the temperature axis. The phase diagram corresponding to this model is shown in figure 1.

3. A classical-proton AIMD model for the free and arrested rotor phases

We have carried out extensive ab initio molecular dynamics simulations on the phase boundaries around Phase I using the CASTEP code with PBE exchange and classical protons. We carry out NPT simulations at 100GPa, starting at 0K in $P6_3/m$. NPT enables us to determine the c/a ratio of hexagonal phases, and the volume changes on transition. The rapid heating rates and finite system size mean that the transition temperatures will be an overestimate of their

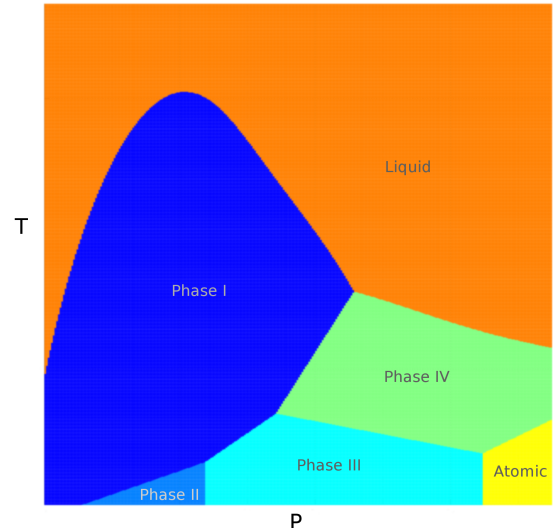


Figure 1. Example phase diagram from the simple packing model Code and parameters used are available in supplemental materials.

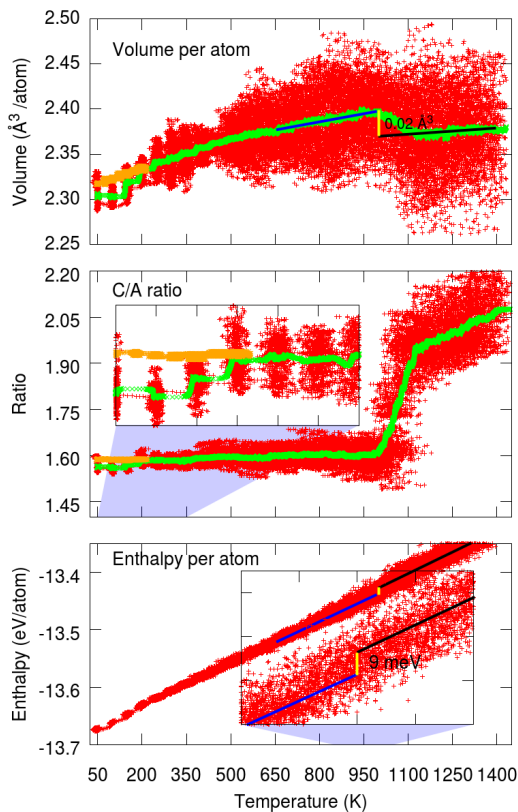


Figure 2. Volume, c/a and enthalpy from a 13.5ps NPT simulation with 288 atoms, 0.5fs timestep, Γ sampling at 100GPa. Thermostat temperature was increased by 50K every 0.5ps. Red crosses depict instantaneous values, light green lines are a 100fs window running average. Orange lines are a running average over a similar simulation with $(4 \times 4 \times 4)$ k -point sampling heated at 25K/150fs. The yellow lines are estimates for the enthalpy and volume drops at melting, obtained from linear regression fits just below and above the melting point.

3.1. k -point convergence

Previous work has reported $Pca2_1$, $P6_3m$ [10] and $P2_1c$ [9] as the most stable structure for phase II. From static relaxations of MD snapshots, we found this stability sensitive to k -point sampling[18]. Here, for phase II identified by EQQ, Γ -only runs favour low c/a ratio whereas at full k -point convergence $P6_3/m$ remains stable until the II-I transition. k -point sampling issues also appear in the melting: sampling with a single k -point we observed melting at 1100K; This calculation is essentially a repeat of previous work[2]. However, using a denser k -point mesh systematically raised the melting point by several hundred degrees.

It is unusual to require dense k -point sampling in molecular crystal, but careful convergence is needed to properly resolve the quadrupole moments in phase II, which are crucial to the ordering. Meanwhile, in the liquid phase, free diffusion allows the atoms to arrange themselves

true thermodynamic values, nevertheless, the phase transitions observed at this level of theory are in qualitative accordance with experiment.

On heating at 100GPa, (figure 2) we observe the II - I transformation at 100K, and melting at 1100K. The close-packed phase I has the lowest density of the three. The phase transitions are evident in movie visualisation. II \rightarrow I is most clearly shown in the angular autocorrelation function (AAF, figure 3a), while melting becomes evident in the mean squared displacement (MSD figure 3c).

Direct measurement of quadrupole interaction energy from the electronic structure is swamped by fluctuations in the MD, but we can measure it via orientational correlations. The quantity EQQ (figure 4) is the interaction energy of two linear quadrupoles pointing in directions, k , k' , separated by a vector r . The molecular quadrupole moment for hydrogen is around $Q = 0.26D\text{\AA}$ [17]. and the ensemble average of EQQ is the quadrupole-quadrupole energy.

$$\langle EQQ \rangle = \langle (3Q^2/4\pi\epsilon_0r^5)[35(k.r)^2(k'.r)^2 - 5(k.r)^2 - 5(k'.r)^2 + 2(k.k')^2 - 20(k'.r)(k.r)(k.k') + 1] \rangle$$

A series of simulations of pressurisation at 600K (Fig 5) showed phase I persisting until about 200GPa at which point it transformed into a disordered structure. The enhanced AAF, indicating the arrest of the rotors, shows this is not a liquid. The disappearance of the strong vibron suggests the structure is similar to the chain-like structure reported elsewhere[18].

AAF, RDF, MSD graphs confirm the broken symmetry - free rotor - liquid sequence with temperature and the weakening of the vibron with increased pressure, followed by extreme broadening and further softening, plus suppression of molecular rotation in Phase III.

in a way most favourable for minimising the Γ -point electron energy at the expense of unsampled contributions from other parts of the Brillouin Zone[18].

3.2. Lattice parameters

Our simulation spontaneously transformed into the hcp structure for phase I. We find the c/a ratio to be essentially independent of temperature, but to decrease with increased pressure from ideal to about 1.57 at 150GPa. This, and the PV equation of state, is in good agreement with the experiment[20].

3.3. Local order

Phase I has no long range order, but the negative $\langle \text{EQQ} \rangle$ (Fig. 4) indicates short ranged order and increasing coupling between the rotors with pressure of a few meV, increasing with pressure approximately as $V^{-\frac{5}{3}}$. The correlation increases as the rotors are become coupled, leading to gradual breakdown in J as a good quantum number. Despite the distinctive signature in spectroscopy[1], this correlation does not become long-ranged and so does not constitute a thermodynamic phase transition.

At low temperature, EQQ is sufficient to cause long-range ordering in the broken-symmetry phase II, with a binding of up to 30meV, enough to be the cause of its stabilisation below 100K.

4. Conclusions

We have presented a model which distills the essential physics determining the phase stability in hydrogen. Phases II and III are energetically favored, through quadrupole interaction and electron delocalisation respectively. Phases I and IV are entropically favoured, primarily due to the high entropy of rotating molecules, which can be understood classically or quantum mechanically. The $J=0$ quantum rotor is an intrinsically large object: the higher compressibility of the liquid compared to phase I can be understood by the increased population of “smaller” molecules in higher energy states.

The success of the classical MD models can be attributed to this near equivalence of quantum uncertainty described by the wavefunction, and classical uncertainty described by the entropy.

The free rotors in phase I become increasingly correlated as pressure increases, due to increased EQQ and steric effect. The many-body wavefunction for this behaviour is not presented here, but clearly the excited states observable in spectroscopy will not have the characteristic overtones of a free rotor. This change in behaviour does not indicate a phase transition.

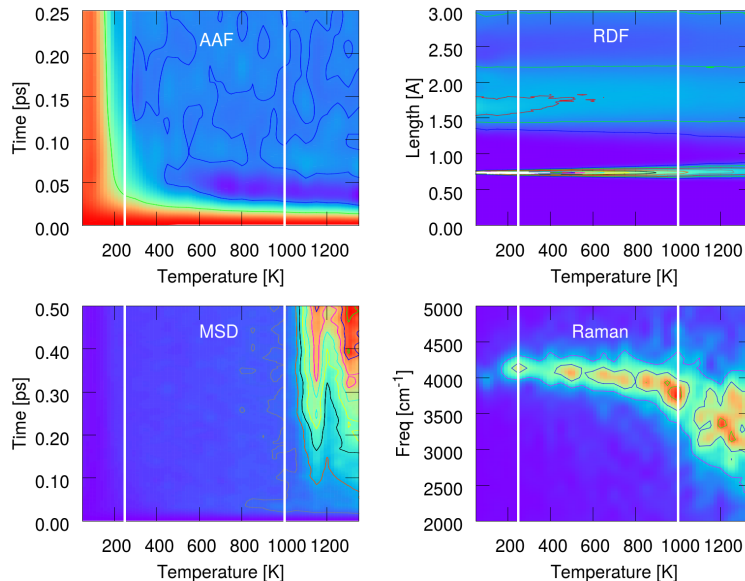


Figure 3. Analysis of heating MD runs at 100GPa (a) AAF vs temperature. Below 150K, in phase II, there is no rotation. Above 150K, in phase I, AAF vanishes within 10 fs, but only at higher temperature, is rotation through 90 degrees free enough to see anticorrelation at 40fs. (b) RDF: Phase II has two molecular neighbours peaks at 1.7 and 2.1 Å, which merge in phase I. All peaks broaden with T. (c) Mean squared displacement is low in Phase II, indicating molecular libration. In Phase I, it is higher due to rotations. Above 1100K, a linear increase in MSD indicates melting. (d) Raman vibron frequency obtained via projection[19], dropping with increasing T, and further at the melting transition. This is consistent with experimental data[4].

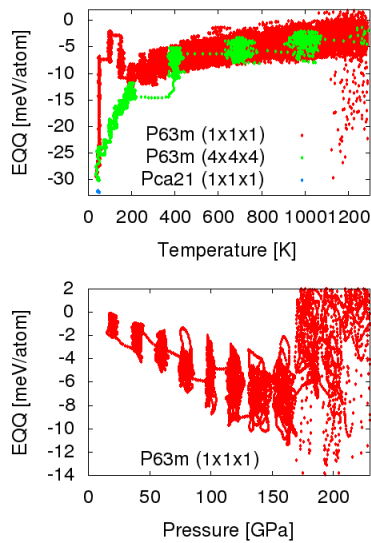


Figure 4. EQQ for heating at 100GPa (top) and pressurising at 600K (bottom). Phase II is unstable with Γ -point sampling (red), but stabilised by slower heating and more k -point sampling (green). The blue dot shows EQQ for $Pca21$.

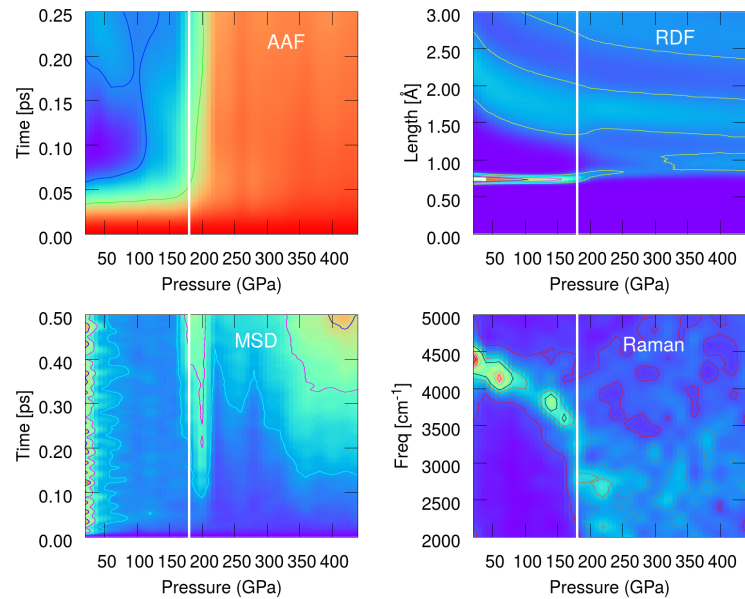


Figure 5. Analysis of pressure dependence at 600K: (a) AAF (b) RDF (c)MSD (d) Raman vs P. Two simulations were started from the equilibrated cell at 100GPa, 600K (phase I) and pressurised/depressurised adiabatically by 20GPa every 0.5ps. The simulations were run with Γ k-point and 288 atoms.

Acknowledgements

We thank EPSRC for support, under UKCP grant K01465X and a studentship for IBM. Additional data including the code for the simple model and MD trajectories can be found at doi.????.????.

References

- [1] Howie R T, Magdău I B, Goncharov A F, Ackland G J and Gregoryanz E 2014 *Phys.Rev.Letters* **113** 175501
- [2] Bonev S A, Schwegler E, Ogitsu T and Galli G 2004 *Nature* **431** 669–672
- [3] Eremets M I and Trojan I 2009 *JETP letters* **89** 174–179
- [4] Howie R T, Dalladay-Simpson P and Gregoryanz E 2015 *Nature materials* **14** 495–499
- [5] Pickard C J, Martinez-Canales M and Needs R J 2012 *Physical Review B* **85** 214114
- [6] Magdău I B and Ackland G J 2013 *Physical Review B* **87** 174110
- [7] Liu H and Ma Y 2013 *Physical Review Letters* **110** 025903
- [8] Eremets M and Troyan I 2011 *Nature materials* **10** 927–931
- [9] Li X Z, Walker B, Probert M I, Pickard C J, Needs R J and Michaelides A 2013 *J. Phys. C M* **25** 085402
- [10] Pickard C J and Needs R J 2007 *Nature Physics* **3** 473–476
- [11] Geng H Y, Song H X, Li J and Wu Q 2012 *Journal of Applied Physics* **111** 063510
- [12] Ackland G J and Magdau I B 2015 *Cogent Physics*
- [13] Magdău I B and Ackland G J 2013 *Physical Review B* **87** 174110
- [14] Caillabet L, Mazevet S and Loubeyre P 2011 *Physical Review B* **83** 094101
- [15] Mao H K and Hemley R J 1994 *Reviews of Modern Physics* **66** 671
- [16] Jackson A and Ackland G 2007 *Physical Review E* **76** 066703
- [17] Orcutt R H 1963 *The Journal of Chemical Physics* **39** 605–608
- [18] Magdau I B and Ackland G 2016 *J. Phys. CP* **this volume**
- [19] Ackland G J and Magdau I B 2014 *High Pressure Research* 198–204
- [20] Loubeyre P, LeToullec R, Hausermann D, Hanfland M, Hemley R, Mao H and Finger L 1996 *Nature* **383** 702–704